

## Simulation of ultrasonic pulse propagation in solids

Rimantas Barauskas and Vytautas Daniulaitis

System Analysis Department, Faculty of Informatics, Kaunas University of Technology

Studentų 50, Kaunas LT 3031, Lithuania

e-mail: rimantas.barauskas@ktu.lt and vytautas.daniulaitis@ktu.lt

### Abstract

Comprehensive understanding of the dynamics of the processes taking place in the testing specimen is available only by solving partial differential equations by finite element or finite differences method. However, even for small practical problems they appear to be of little effectiveness because of great computer resource (time and memory) usage. The situation can be improved by developing efficient algorithms of numerical modelling, based on a deeper analysis of the wave propagation phenomenon. As a result of the analysis, the finite element procedure in regular and free triangular finite element meshes was developed and adopted for the short wave propagation modelling during the ultrasonic measurement processes.

*Keywords: finite element method, explicit analysis*

### 1. Introduction

Ultrasonic non-destructive testing (NDT) is playing an increasingly important role for the reliability and safety of various components and systems. Ultrasonic waves are mechanical vibrations and therefore ultrasonic testing is especially suited to detection of elastic anomalies and measures of physical properties such as porosity, structure and elastic constants. Examples of the ultrasonic NDT applications include mill components (rolls, shafts), jet engine components (turbine blanks and compressor rotors), airframe (frame section), rolling stock (axles, wheels) railroad track maintenance and many others. Ultrasonic testing instrumentation is basically electronic and indications may be obtained in real time. This characteristic permits rapid scanning with automatic positioning, plotting and alarming.

The wide range of applications of the method creates the need of understanding the physics of the ultrasonic testing measurement processes by means of mathematical modelling and simulation of ultrasonic testing and measurement processes. The distinguishing feature of ultrasonic measurements is that the object testing scheme has to be designed individually for different applications. The reflected amplitude is commonly used for the defect sizing in ultrasonic NDT. However very often there are many serious limitations, because the reflected ultrasonic pulse is subjected to variations due to coupling factors, reflectivity, angle or roughness of the defect and to interference effects. That is why a good model is always appreciated for the development of the testing procedures, for parametric studies or for the qualification of testing procedures.

In this study we focus our attention on transient behaviour of the propagation of the typical ultrasonic pulse excited on the boundary of the environment. During the last decade a huge effort has been made to create the techniques and software able to solve realistic problems of ultrasonic wave propagation. The available publications on the problem present several different approaches. The finite difference schemes able to associate different density and elastic parameters with each grid point, to take into account the boundaries between different materials and arbitrary geometrical shape of the region are referenced in [1]. The approach has been implemented as WAVE2000 computational ultrasonics software able to solve 2D problems in powerful multiprocessor computing environments, as well as, in

PC's. The approach is based on efficient algorithms of step-by-step computation of the structural displacements over all the structure and the time interval. 17 mesh points per shortest wavelength have been used, and the time step, ensuring the stability of the explicit time-marching scheme has been estimated as  $\Delta t \leq \frac{\Delta x}{\sqrt{v_l^2 + v_t^2}}$ , where  $v_l, v_t$  - velocities of the

longitudinal and shear elastic waves. The stability of the explicit numerical integration scheme being ensured, the accuracy requirements are usually satisfied as well - with 17 points per wavelength the maximum free vibration frequency represented by the structural model is usually much higher than the highest harmonic component of the wave of interest. The combination of finite difference and finite element approach has been earlier described in [2].

The three-dimensional problems seem to be most realistic to approach by using the boundary integral equation techniques the transient formulations and implementation of which have been mentioned in [3] for acoustic and in [4] for elastic waves. The space and time step requirements are similar as mentioned above for the finite difference approach, however, only surface of the body has to be discretized. Moreover, adaptive meshing can be employed by using refined meshing in the vicinity of geometrical irregularities. The best results can be expected by combining properly the finite element and boundary element approaches. The boundary integral method is very efficient for presenting the homogeneous regions, however, the sources of numerical instabilities, excessive oscillations of the solution and the measures to cope with them at present are not so clearly understood as for the finite element models. On the other hand, the zones containing non-homogeneous materials are much easier to represent by using finite element models.

This work aims to analyse the finite element models for transient elastic wave propagation. In uniform finite element models containing identical rectangular elements the solution algorithms are very similar to those used in finite difference schemes as no structural matrices are necessary to assemble and calculation formulae for each grid point can be easily written. On the other hand, it is easy to couple such models with regions described by means of free finite element meshes, as well as, by boundary element models. It has been shown in [5], [6] that dispersion relations of uni-dimensional finite element models can be significantly improved by selecting appropriate form of

the mass matrix. As a consequence, only 5-7 elements per wavelength instead of 17 often suffice to represent satisfactory the wave propagation law. As contraindication for using such an approach is a non-diagonal form of the mass matrix requiring to use iterative methods for solving the linear algebraic equation system at each time step. However in 2D and 3D cases more than 3 times increase of the element size result in considerable savings in computational time even if iteration at each time step is necessary. Estimation of the conventional methods' effectiveness shows that neither of them is optimal for the ultrasonic NDT simulation. This paper is addressed to the development of the fast computer algorithms. As a consequence of the investigation the computer software for simulation of 2-D plain stress, plain strain and axi-symmetric models has been created.

## 2. Model building strategy

Ultrasonic wave propagation phenomenon has a set of the features distinguishing it from the other problems. Namely, the length of the propagating ultrasonic pulse is up to several hundred times smaller than the spatial dimensions of the body where vibrations take place in. In general defects, complicated boundary geometry (drilled holes, chamfers) are solitary instances in the structure. Regarding to the ultrasonic signal wavelength, the model could be treated as a composition of some large homogenous areas. They are being discretized by uniform quadrilateral finite element mesh which ensures solution precision and stability. The *central difference* time integration scheme in such meshes can be reduced to a recursive formula by which the displacement of each node is computed by using displacements of adjacent nodes. Global matrices of the structure do not have to be assembled since all finite elements are identical and solution for displacements is carried out by well known technique [9] at the element level. Since the homogenous areas dominate in the structure, significant savings of the computer resource are achieved.

Boundary regions of the specimen are presented by the triangular finite element mesh. If the boundary region leaning to the quadrilateral finite element area has a triangular shape it is being meshed by uniform triangular mesh and recursive formula for the solution is implemented. If the boundary region is of arbitrary shape, it is meshed by a free triangular finite element mesh. For freely meshed domains we assemble the structural matrices, however, the size of freely meshed zones is usually small in comparison with large regularly meshed domains. As a result, the model is built in brick-wise manner of rectangular, triangular and polygonal zones (Fig.1).

In practice, the division of the domain into rectangular, triangular and polygonal zones is performed as follows. The rough rectangular grid is put on the model. Area entirely overlapped by the grid cells is considered to be the rectangular finite element mesh zone. Areas partially overlapped by cells

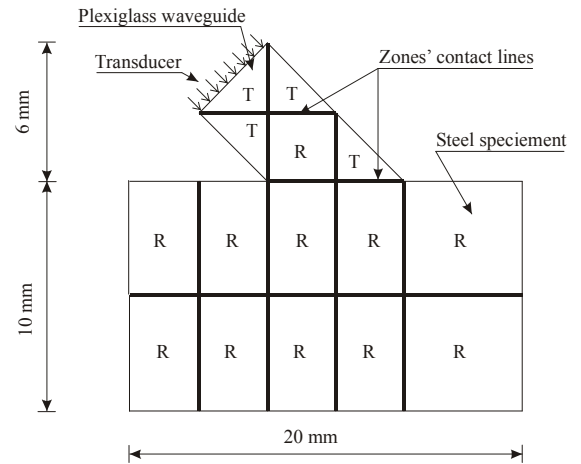


**Fig.1** Scheme of the model division into rectangular and triangular zones.

Note: 'T' corresponds to the triangular, 'R'- to the rectangular zones.

are considered to be triangular or polygonal zones and are meshed by free or regular triangle elements. If the cell happens to be outside of the model, it is an empty zone. Orientation of the rough grid usually is aligned to the vertices of the model in order to obtain the reasonable division into zones, i.e., minimum number of the triangular and maximum number of the rectangular zones. The spacing of the lines of the rough grid is variable in order to facilitate the division.

Solution for displacements is calculated separately for each individual zone. The fact that zones are being processed separately permits to control model size during the computation. Actually, after the time instant of excitation the wave pulse propagates in the structure gradually with constant wave velocity (Fig.2).

During the first stage of the pulse propagation the non-zero displacements are residing in a very small part of the model, while the rest of the model can be excluded from the calculation. The effective model size grows as the time goes on and is defined by the geometric shape of the wave frontline. Practically, the size of the active part of the model is controlled by supplying the "activity index" to all zones. Zones which are not reached by wave front are inactive and calculations are not performed upon them since all displacements are zero.

If a zone of the computational model contains only small residual vibrations or isolated wave pulses of no practical interest, it is marked as inactive as well. We assume the displacement to be zero if it does not exceed  $10^{-4} \times u_{\max}$ , where  $u_{\max}$  - the maximum value of the displacement since the start of simulation. The technique also enables to eliminate the "numerical noise" the propagation velocity of which is at least two times greater as the speed of the longitudinal wave.

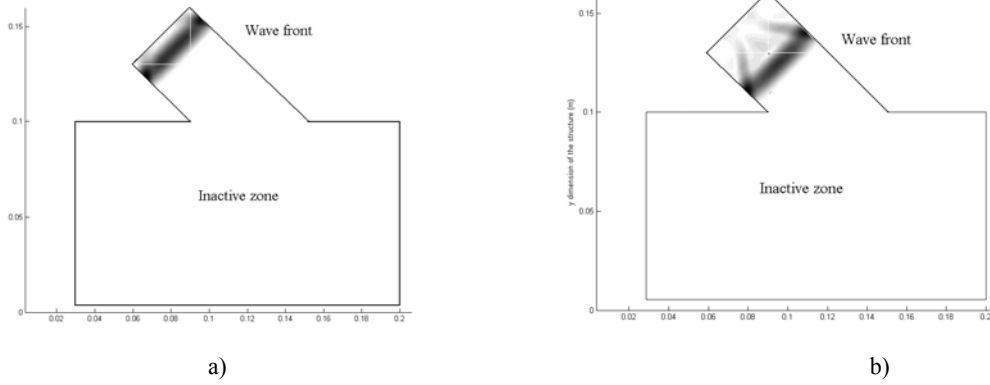


**Fig.2** Wave front propagation in the structure: a) step number 80, b) step number 200

Another advantage gained in the model division into the different zones is the possibility to use individual mesh for each separate zone. This technique is efficient for simulation of waves in multi-material models. The materials of low wave propagation velocity provoke the unnecessarily refined mesh also in the high wave velocity materials. The use of the different meshes significantly reduces total number of the nodes of the model. The differently meshed zones are fitted within the model by interpolating the nodal displacements on the contact lines between the zones.

Time sub-stepping technique enabling to use different time integration steps in differently meshed zones presents another source for the efficiency increase of the program. It is under development now.

The discussed features of the ultrasonic pulse propagation make possible to develop an efficient algorithm of computation. The explicit time integration scheme in uniform finite element meshes is combined with the conventional finite element technique in free meshes. The use of efficient explicit time integration schemes combination of different size and time steps result in significant savings of computer resources and high performance.

### 3. Application of the finite element method and algorithmic realization

Elastic wave propagation analysis is performed by solving the structural dynamic equation

$$[M]\{\ddot{U}\} + [C]\{\dot{U}\} + [K]\{U\} = \{F(t)\}; \quad (1)$$

where  $[M]$ ,  $[K]$ ,  $[C] = \alpha[M]$  - the mass, stiffness and proportional damping matrices;  $\{F\}$  - the external load vector,  $\{U\}$ ,  $\{\dot{U}\}$ ,  $\{\ddot{U}\}$  - are the nodal displacement, velocity and acceleration vectors of the structure.

The time integration is being performed by means of the *central difference* integration scheme:

$$\{U_{t+\Delta t}\} = [\hat{M}]^{-1} \left[ \{F_t\} - \left( [K] - \frac{2}{\Delta t^2} [M] \right) \{U_t\} - [\tilde{M}] \{U_{t-\Delta t}\} \right] \quad (2)$$

where

$$[\hat{M}] = \frac{1}{\Delta t^2} [M] + \frac{1}{2\Delta t} [C] = \frac{1}{\Delta t^2} [M] + \frac{1}{2\Delta t} \alpha [M];$$

$$[\tilde{M}] = \frac{1}{\Delta t^2} [M] - \frac{1}{2\Delta t} [C] = \frac{1}{\Delta t^2} [M] - \frac{1}{2\Delta t} \alpha [M],$$

$\Delta t$  - the time integration step.

From (2) we obtain:

$$\begin{aligned} \{U_{t+\Delta t}\} = & [\hat{M}]^{-1} \{F_t\} - [\hat{M}]^{-1} [K] \{U_t\} + \\ & + \frac{2}{\Delta t^2} [\hat{M}]^{-1} [M] \{U_t\} - [\hat{M}]^{-1} [\tilde{M}] \{U_{t-\Delta t}\} \end{aligned} \quad (3)$$

Displacement vector  $\{U_{t+\Delta t}\}$  is evaluated by using assembled zone's matrices, however in the case of the lumped mass matrix and regular finite element mesh formula (3) is actually applied for every individual node. Only the product  $[K]\{U_t\}$  for a node should be obtained on the element level and then assembled to the nodal force vector. Since all regular finite elements in the rectangular or triangular zones are identical, multiplication of the structural matrices by nodal displacement vectors can be presented by a simple and fast recursive formula. Calculation of the product corresponding to a rectangular finite element mesh node  $ij$ , see Fig. 3, can be presented as

$$\begin{aligned} [K]\{U\}_{i,j} = & ([K_{11}^e] + [K_{22}^e] + [K_{33}^e] + [K_{44}^e])\{U\}_{i,j} + \\ & + ([K_{21}^e] + [K_{34}^e])\{U\}_{i-1,j} + ([K_{23}^e] + [K_{14}^e])\{U\}_{i,j+1} + \\ & + ([K_{12}^e] + [K_{43}^e])\{U\}_{i+1,j} + ([K_{41}^e] + [K_{32}^e])\{U\}_{i,j-1} + \\ & + [K_{24}^e]\{U\}_{i-1,j+1} + [K_{13}^e]\{U\}_{i+1,j+1} + \\ & + [K_{42}^e]\{U\}_{i+1,j-1} + [K_{31}^e]\{U\}_{i-1,j-1}, \end{aligned} \quad (4)$$

where  $[K_{st}]$ ,  $s, t=1,2,3,4$  are blocks of dimension  $2 \times 2$  of the stiffness matrix of the quadrilateral element the local nodal numbers of which are being assigned from the bottom left corner in counter-clockwise direction. In the case of plain stress and plain strain models, the stiffness matrices in the rectangular zone are identical, therefore in the formula (4) the superscripts are omitted.

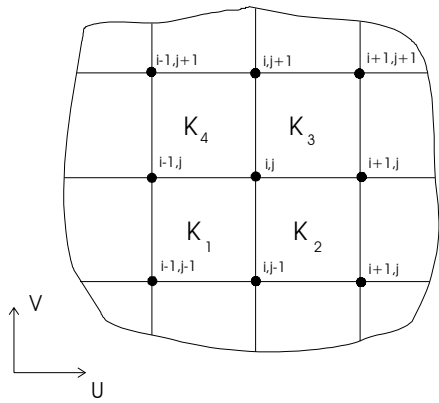


**Fig.3** Fragment of a quadrilateral finite element mesh

For the regular triangular finite element mesh formula (4) for the product  $[K]\{U_i\}$  of the node  $ij$  (see Fig.4) reads as

$$\begin{aligned}
 [K]\{U\}_{i,j} = & \left( [K_{22}^{1e}] + [K_{33}^{2e}] + [K_{33}^{3e}] + [K_{11}^{4e}] + [K_{11}^{5e}] + [K_{22}^{6e}] \right) \{U\}_{i,j} + \\
 & \left( [K_{32}^{2e}] + [K_{31}^{3e}] \right) \{U\}_{i-1,j} + \left( [K_{13}^{5e}] + [K_{23}^{6e}] \right) \{U\}_{i+1,j} + \\
 & \left( [K_{32}^{3e}] + [K_{12}^{4e}] \right) \{U\}_{i,j+1} + \left( [K_{23}^{1e}] + [K_{21}^{6e}] \right) \{U\}_{i,j-1} + \\
 & \left( [K_{13}^{4e}] + [K_{12}^{5e}] \right) \{U\}_{i+1,j+1} + \left( [K_{21}^{1e}] + [K_{31}^{2e}] \right) \{U\}_{i-1,j-1} \quad (5)
 \end{aligned}$$

where  $[K_{st}^{le}]$ ,  $l, s, t = 1, 2, 3$  - are the blocks of stiffness matrix of the triangular finite element. Here we have two different types of the stiffness matrices, because zone is meshed by the triangles, which have two different orientations. Since all the triangles have identical shape (the angles and vertices) they have to have the same stiffness in local references. The transformation from the local coordinates to the global ones result only in the position change of the matrix blocks. For the plain stress and plain strain models it sufficient to store only one version of the element stiffness matrix.

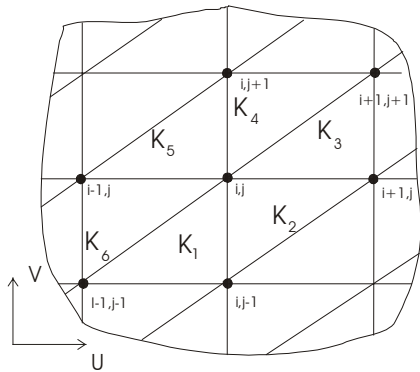


**Fig.4** Fragment of a triangular finite element mesh

The calculation of the displacements for freely meshed domains requires considerably greater amounts of the computational resources, however, the number of nodes in such domains is usually small in comparison with the total number of nodes of the model. Vector  $\{U_{i+\Delta t}\}$  for freely-meshed zones is evaluated by means of formula (3) where structural matrices of zones are used.

The derived recursive formulae (4) and (5) run correctly for the zone's inner nodes. For the zone's corner and peripheral nodes, which at the same time are the peripheral nodes of the model, (4) and (5) have to be modified. The latter nodes do not have a full set of neighbouring nodes, therefore the stiffness matrix blocks, corresponding to the dummy nodes have to be nullified. When calculating displacements of the nodes, located on contact lines or corners, the displacements of the neighbouring zone nodes should be used.

Since zones are processed individually and only one per time, the sums of products  $[K]\{U_i\}$  are accumulated for nodes on each interface line (skeleton in bold face, see Fig.1). During each time integration step we loop through the zones and assemble the products  $[K]\{U_i\}$  for each interface node due to all neighboring zones. After that the zones are processed individually.

In multi-material structures, the different mesh density for each material is employed. Generally, the positions of interface nodes of two differently meshed zones do not coincide. The procedure for the traction forces evaluation and the displacement increment calculation (second term in the formula (3)) are modified as follows. Before the time integration stage, the mass on the contact line is scaled to the smallest element size and stored as a nodal mass vector. The solution for displacements is being found for a smaller discretization step and then approximated for the rough mesh on the contact line.

Once the diagonal matrices  $[\hat{M}]$  and  $[\tilde{M}]$  have been already formed, during each time step the product  $[K]\{U_i\}$  of the rough mesh have to be converted to the space step of the finer mesh. Traction forces of the rough mesh are replaced by the equivalent distributed loading, which is transferred to the finer mesh nodes and converted to the corresponding traction forces (see Fig. 5).

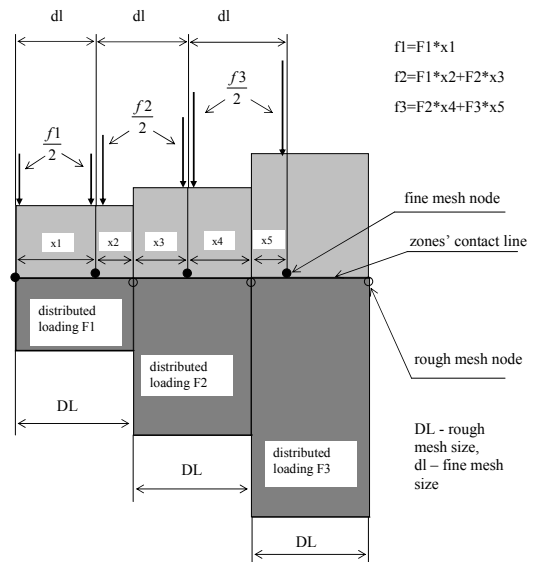


**Fig. 5** Calculation of the traction forces on the different mesh contact line

The quantity  $\frac{[K]\{U_i\}}{m_{node}}$  is a displacement increment, which is being found for a finer mesh. A Lagrangian interpolation is

used in order to reconstruct the solution for rough finite element mesh from a solution in finer mesh (see Fig. 6).

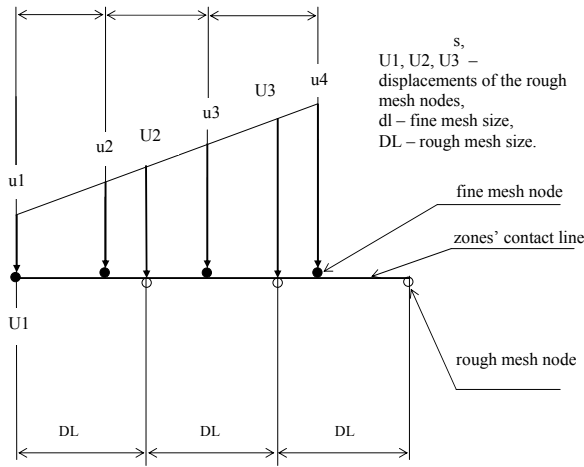


Fig.6 Displacements reconstruction for rough mesh zone

The third and fourth terms in (3) have not to be re-evaluated for the contacting nodes, because quantities  $\frac{m_{node}}{\hat{m}_{node}}$  and  $\frac{\tilde{m}_{node}}{\hat{m}_{node}}$  are constant for the nodes on the interface line. It is sufficient to multiply displacement vectors by  $\frac{m_{node}}{\hat{m}_{node}}$  and  $\frac{\tilde{m}_{node}}{\hat{m}_{node}}$  for rough and fine mesh nodes correspondingly in order to obtain the solution.

Two dimensional axisymmetric finite element models require more storage, as the element mass matrix  $[M]$  and stiffness matrix  $[K]$  are functions of the element radial position. If the uniform finite element mesh is being used, the model contains  $n$  different finite element matrices, where  $n$  denotes number of the finite elements in one-element width stripe from minimum to maximum radius. Having saved the matrices of these finite elements the above discussed algorithm has been adopted for ultrasonic wave propagation problems in axisymmetric solids. In the case of the quadrilateral finite element mesh, finite element pairs  $[K_1]$ ,  $[K_4]$ , and  $[K_2]$ ,  $[K_3]$  occupy different radial positions and finite element matrices  $[K_1], [K_2], [K_3], [K_4]$  are no longer identical (Fig. 3). By using two types of the finite element matrices  $[K_1]$  (here  $[K_1] = [K_4]$ ), and  $[K_2]$  (here  $[K_2] = [K_3]$ ) formula (4) is being adopted for the axisymmetric model investigation. For triangular finite element mesh also two types of the stiffness matrices  $[K_1]$  and  $[K_3]$  have to be used in formula (5).

It may be expected that axisymmetric models require huge amounts of storage for the stiffness and mass matrices of the elements. However, storage optimisation was made by employing

a stiffness and mass matrices reproduction procedure described below.

For the axisymmetric models matrices  $[M]$  and  $[K]$  are linear functions of the finite element radial position. Element-by-element subtraction of two adjacent finite element stiffness (mass) matrices provides us the variations of the stiffness (mass) matrix elements. Next we have to evaluate the matrices of the finite element, occupying the minimal radial position. Once we have the variations and the matrices of the finite element located at the minimal radius, the matrices of the rest finite elements can be easily computed. For the quadrilateral finite element the necessary amounts of storage are determined by 10  $2 \times 2$  blocks  $[K_{st}^e]$  (instead of  $4 \times 4 = 16$  blocks), and 7 blocks of the directional coefficient storage. The total amount of storage necessary for the stiffness matrices of the axisymmetric model is  $10 \times 4 + 7 \times 4 = 68$  real numbers – slightly more than it is necessary for one quadrilateral finite element ( $8 \times 8 = 64$ ). The numerical experiment demonstrates that the stiffness matrix reconstruction from the saved blocks and coefficients runs even faster than procedure when all necessary stiffness matrices are formed and stored. The model simulation time was 281 and 262 minutes for the first and second case respectively. In both cases model was defined by 122672 nodes and 10000 time integration steps.

#### 4. Simulation results

In this section the test results of the algorithm efficiency and an example of the problem solution are presented.

The plexiglass-steel specimen presented in Fig. 1 was examined three times using different finite element meshes. In the first case all the model was meshed by the meshes of the same space step sizes. Rectangular zones were discretized by the uniform quadrilateral finite elements, and triangle zones – by free triangular finite element mesh. The finite element size was predetermined by the longitudinal wave velocity in the plexiglass region and was equal to 0.00018 m. The model size was 590,000 nodes. Simulation time in all cases was set to 10,000 time steps. The simulation was carried out on a 1.7 MHz Pentium IV computer and took 1054 minutes. In the second trial, adaptive meshing was used. Finite element size for steel and plexiglass domains were set to 0.00034 m. and 0.00018 m. respectively. Rectangular and triangular zones were meshed by the uniform quadrilateral and free triangular finite element meshes respectively. Model was presented by 190,000 nodes, and simulation time was 321 minutes. The last simulation was performed with the model entirely meshed by the regular quadrilateral and triangular finite element meshes. Finite element sizes were 0.00034 m. for steel, and 0.00018 m. for plexiglass regions. Simulation took 289 minutes. Simulation results are presented in the Fig.7.

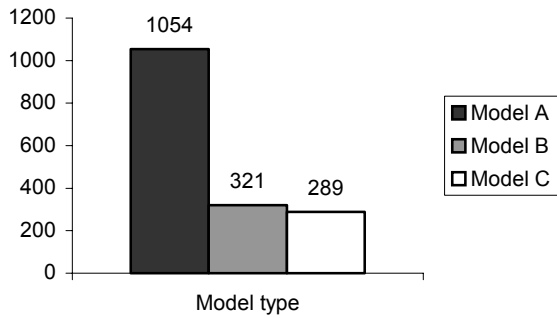


**Fig.7** Model processing time.

*Model A* – fixed size regular quadrilateral and free triangular finite element meshes;

*Model B* – adaptive mesh, regular quadrilateral and free triangular finite element meshes;

*Model C* – adaptive regular finite element mesh.

Fig.8 presents the total displacement plot for a steel-plexiglass model at the time instant  $23 \mu\text{s}$  when the wave front reaches the steel-plexiglass contact line and enters the steel region. On the contact line wave diffraction and reflection is observed.

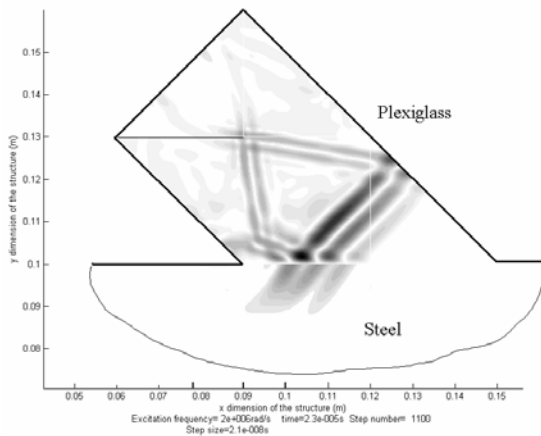


**Fig. 8** Displacement plot at the time  $23 \mu\text{s}$ .

Note: Displacements of the steel region are magnified 3 times in order to be observables

## Conclusions

This paper is addressed to the problems of the finite element modelling of the transient ultrasonic pulse propagation. Due to requirements imposed on the space and time steps, the dimensions of the finite element models become very large. The simulation algorithm was optimized by taking into account the practical features of the ultrasonic measurement procedures. The simulation effectiveness has been improved by employing the computational strategy allowing to control the size of the active part of the model, filtrating the numerical noise and combining the domains meshed by different space step sizes in the same model. The algorithm works with 2D and axisymmetric models.

## References

- [1] Shechter, R.S., Chaskelis, H.H., Mignona, R.B., Delsanto, P.P., Real-Time Parallel Computation and Visualization of Ultrasonic Pulses in Solids, *Science*, 265, 1188-1192.
- [2] Harumi, K. 'Computer simulation of ultrasonics in a solid', *NDT International*, 19,N.5, 315-332, (1986).
- [3] Bluck, M. J. and Walker,S.P., Analysis of three-dimensional transient acoustic wave propagation using the boundary integral equation method, *Int. J. Num. Meth. Eng.*, 39, 1419-1431, (1996).
- [4] Han, S. and Ichikawa, Y., Numerical modelling for scattering of waves in three dimensional cracked material, *Int. J. Num. Meth. Eng.*, 38, 4081-4100, (1995).
- [5] Barauskas, R. and Daniulaitis, V., Modelling techniques for ultrasonic wave propagation in Solids, *Ultragarsas*, N1(29),(1998).
- [6] Daniulaitis, V. and Barauskas, R., Modelling techniques for ultrasonic wave propagation in solids:2D case, *Ultragarsas*, N2(30),7-10,(1998).
- [7] Morse, P. And Feshbach, H., *Methods of Theoretical Physics, Parts I&II*, McGraw-Hill, New-York,(1953).
- [8] Zienkiewicz, O.C., *The Finite Element Method, IV edition, Volumes I&II*, McGraw-Hill, London, (1989).
- [9] Bathe,K.J., *Finite Element procedures in Finite Element Analysis*, Prentice Hall, Englewood Cliffs, N.J.,(1987).
- [10] Katona, I. and Zienkiewicz,O. C., 'A unified set of single step algorithms, Part 3: the beta-m method, a generalization of the Newmark's scheme', *Int. J. Num. Meth. Eng.*, 21, 1345-1359, (1985).
- [11] Pezeshk, S. and Camp, C.V., An explicit time integration technique for dynamic analyses, *Int. J. Num. Meth. Eng.*, 38, 2265-2281, (1995).